biosensors

MDPI

Review

SAM-Support-Based Electrochemical Sensor for Aβ Biomarker Detection of Alzheimer's Disease

Phan Gia Le [1], Hien T. Ngoc Le [1], Hee-Eun Kim [2] and Sungbo Cho [1,3,*]

[1] Department of Electronic Engineering, Gachon University, Seongnam-si 13120, Republic of Korea; legiaphan2020@gachon.ac.kr (P.G.L.); ngochien1809@gmail.com (H.T.N.L.)
[2] Department of Dental Hygiene, Gachon University, Incheon 21936, Republic of Korea; hekim@gachon.ac.kr
[3] Department of Health Sciences and Technology (GAIHST), Gachon University, Incheon 21999, Republic of Korea
* Correspondence: sbcho@gachon.ac.kr; Tel.: +82-(31)-750-5321

Abstract: Alzheimer's disease has taken the spotlight as a neurodegenerative disease which has caused crucial issues to both society and the economy. Specifically, aging populations in developed countries face an increasingly serious problem due to the increasing budget for patient care and an inadequate labor force, and therefore a solution is urgently needed. Recently, diverse techniques for the detection of Alzheimer's biomarkers have been researched and developed to support early diagnosis and treatment. Among them, electrochemical biosensors and electrode modification proved their effectiveness in the detection of the Aβ biomarker at appropriately low concentrations for practice and point-of-care application. This review discusses the production and detection ability of amyloid beta, an Alzheimer's biomarker, by electrochemical biosensors with SAM support for antibody conjugation. In addition, future perspectives on SAM for the improvement of electrochemical biosensors are also proposed and discussed.

Keywords: Alzheimer's disease; electrochemical detection; self-assembled monolayer; nanomaterials

Citation: Le, P.G.; Le, H.T.N.; Kim, H.-E.; Cho, S. SAM-Support-Based Electrochemical Sensor for Aβ Biomarker Detection of Alzheimer's Disease. *Biosensors* **2023**, *13*, 809. https://doi.org/10.3390/bios13080809

Received: 5 July 2023
Revised: 1 August 2023
Accepted: 9 August 2023
Published: 11 August 2023

1. Introduction

Nowadays, Alzheimer's disease (AD) is receiving increasing attention as its burden on society due to memory and recognition impairment relating to neurodegeneration [1]. Based on statistical data, in 2020, the number of Alzheimer patients was estimated to be around 50 million and is predicted to be roughly 152 million by 2050 [2]. The expenditure for serving AD patients is about USD one trillion annually [2]. Thus, reducing the number of patients and the economic burden is extremely necessary.

AD, like Parkinson's disease, is linked to neurodegeneration [3,4]. The illustration of brain images observed from Alzheimer's patients is described in Figure 1. There are many hypotheses about the formation of this disease; the appearance of the amyloid-beta oligomer (AβO) tangle and fibrils in the brain derived from Aβ aggregation has been widely accepted by numerous researchers, as documented by high Aβ concentrations in human blood and cerebrospinal fluid (CSF) obtained from clinical research [1]. Thus, the biomarker of Amyloid beta protein ($A\beta_{1\text{-}40}$ and $A\beta_{1\text{-}42}$), phosphorylated tau (p-tau) aggregation, causes neurotoxicity [4,5]. The production of Aβ originates from the cleavage of the amyloid precursor protein (APP) by β- and γ-secretase, whereas cleavage by α-secretase is non-amyloidogenic [1]. The progress of Aβ formation occurs in two steps: first, β-secretase cleaves APP to form C99; next, γ-secretase continues cleaving C99 to generate Aβ of a different length, consisting mainly of $A\beta_{40}$ and $A\beta_{42}$, as presented in Figure 2. An insignificant number of researchers have studied acetylcholine esterase, acetyl choline, and choline as biomarkers associated with AD [2,6–9]. Biosensors capable of detecting these biomarkers for diagnosis and early warning to support AD treatment have been intensively researched currently. Thus, circumventing maintaining challenges in AβO-based biosensors will be crucial in enabling the diagnosis and treatment of AD.

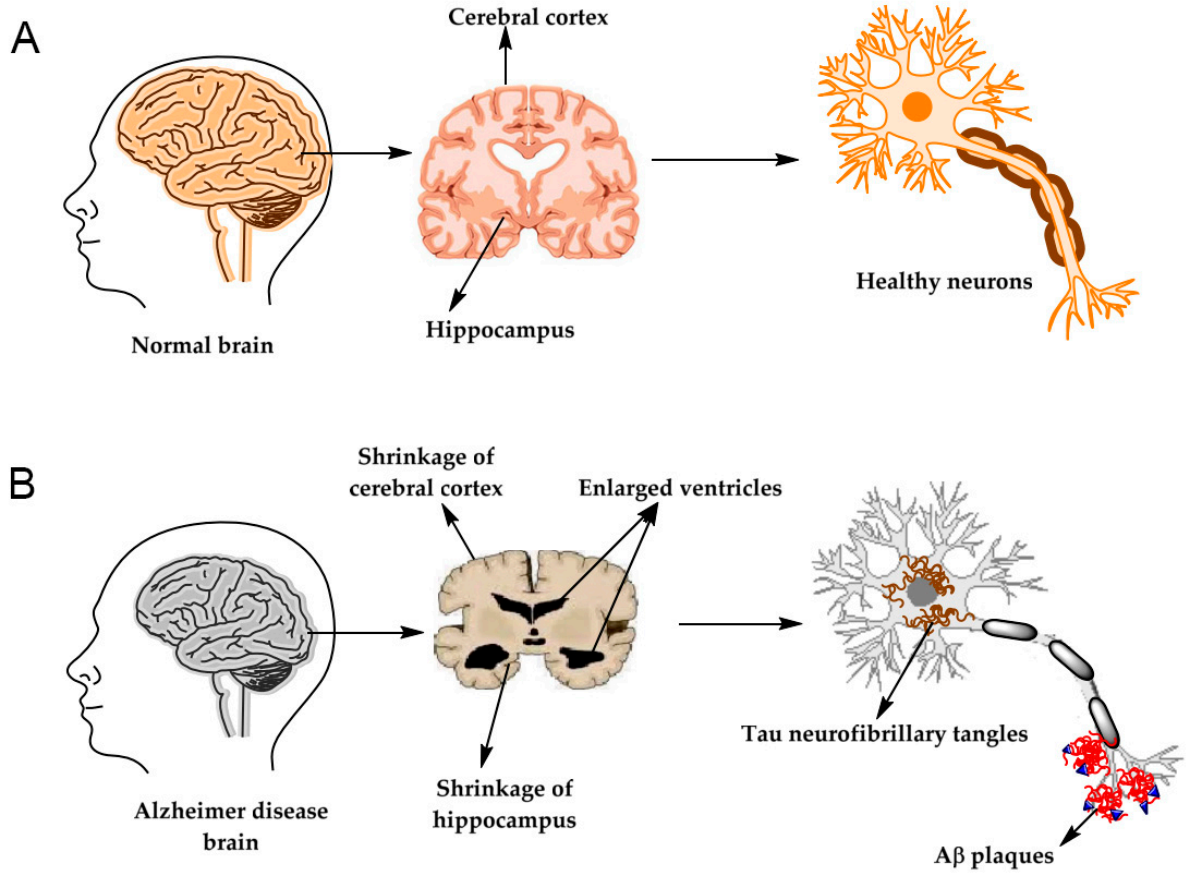

Figure 1. Illustration of the brain and neurons structures for both cases of (**A**) brain of a healthy person and (**B**) brain of a person with Alzheimer's [2].

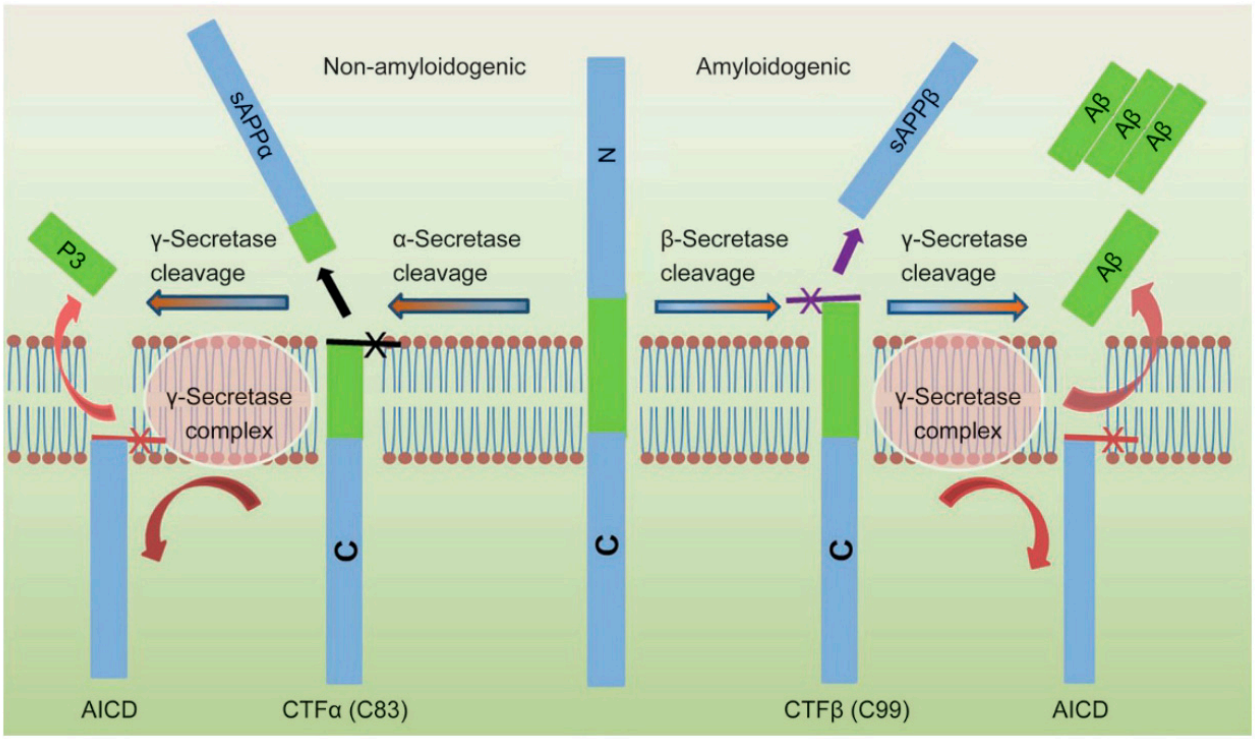

Figure 2. Mechanism for the Aβ peptides formation from human APP proteolysis [10].

Research on the detection of AβO has taken diverse approaches, such as conventional [11–14], optical [15–18], electrochemical [19–21], and electroluminescent methods [22–25], and quartz crystal microbalance [26–28]. Among these, conventional detection methods utilize magnetic resonance imaging (MRI) [13,14,29], near-infrared fluorescent (NIRF) [16,30,31], and positron emission tomography (PET) [11,12,32,33], which are time-consuming, have low spatial resolution [34], and are also expensive as well as cause side effects such as vomiting, flushing, itching, headache, and nausea [4]. In contrast, the colorimetric method has the pros of visualization, a low cost, and easy operation, but the high limit of detection (LOD) makes it not useful enough for Aβ biomarker detection [35–37]. However, the fluorescent method sometimes enables improvement in the LOD at the picomolar or femtomolar level [38,39]. Electrochemical sensors are well-known for their quick reaction rate, high precision, high sensitivity, good controllability, and instantaneous responsibility [40]. Moreover, the fabrication of electrochemical sensors is straightforward, pre-treatment of a clinical sample is not required, and sample volume is insignificant [41]. In addition, it has a wide range of applications, namely clinical diagnosis, biomedical research, food quality management, and environmental monitoring [42]. Especially, electrochemical sensors are compatible with miniaturized devices, which are appropriate for detecting biomarkers with an ultra-low concentration in human serum [43,44], saliva [45,46], blood [47,48], CSF [49,50], and plasma [51–53]. The operation of Aβ-based electrochemical sensors related to AD has been reported by a significant number of scientists obtaining high sensitivity and selectivity.

A self-assembled monolayer (SAM) has been applied in chemical sensors, biosensors, batteries, and electronic devices [54–56]. In electrochemical sensors, SAM is presented as a conjunction layer on the working electrode surface, which is subjected to electrode modification towards improvement in sensor selectivity and sensitivity relying on functionalities for immobilizing and orientating enzymes and antibodies [4,34,57–59]. So, an SAM-appropriate design and fabrication can enhance electrochemical sensor performance. In addition, reported SAM-based electrochemical sensors for Alzheimer's biomarker detection obtained an ultralow detection limit, which reflects that the utilization of SAM is suitable in the development of such electrochemical sensors. To the best of our knowledge, no publication has discussed the SAM of modified electrodes for Aβ peptide detection. Therefore, the current review presents and discusses SAM-related electrochemical sensors. The trends and challenges of electrochemical sensors are also discussed.

2. Overview of Electrochemical Sensors

2.1. Electrochemical Sensor Architecture

An electrochemical sensor is an electrical equipment module which receives electrical signals derived from biochemical reactions taking place between molecules, which is a redox progression [4,60]. Basically, electrochemical sensor architecture consists of three electrodes: the working electrode, reference electrode, and counter electrode [40]. Among these, the working electrode is a crucial component, as the main reaction occurs on its surface, and thus it determines the sensitivity, selectivity, and durability of the sensor. Many kinds of working electrodes have been developed to enhance the selectivity and sensitivity of Aβ electrochemical sensors; these include glassy carbon electrode (GCE) [53,61], paper-based carbon electrode [62,63], screen-printed electrode (SPE) [64], Ni-foam electrode [65], and interdigitated microelectrode [4,34,57,66,67]. Amongst these, GCE is very popular but not suitable for miniaturized devices, paper-based carbon electrode is inexpensive and disposable, screen-printed and Ni-foam electrodes are easily fabricated, and interdigitated microelectrode is highly sensitive but requires a prohibited machine and trained technician. Pristine working electrodes for electrochemical sensors with intrinsic physiochemical properties hinder the detection of the Aβ biomarker, which can be improved by tailoring one or many layers of materials on the surface, such as novel metal [62,63], carbon [61,64], composite [68,69], or a conductive polymer [70] to boost the sensor's sensitivity. Generally, electrochemical electrodes are expensive, whereas they possess higher sensitivity than other reported method counterparts [69,71], which meets the requirements for biomedical

application. In addition, the expenditure of electrochemical sensor production can be reduced by scaling up; specifically, paper-based screen-printed electrodes are thin, easy to fabricate, not time-consuming, easily mass-produced, highly economical, and disposable, which will be crucial to point-of-care systems in the future. Hence, suitably modified electrodes can improve the detection of the Aβ biomarker down to an ultra-low level in human serum, saliva, CSF, and plasma.

2.2. Operational Principle

Electrochemical sensor operation is based on the redox reaction of the analyte on the working electrode surface accompanied by electrical signal generation, which varies with different analyte concentrations [72–74]. The signal is received by the detector of the analyzer, e.g., voltammetry analyzer, impedance analyzer, and so on. Changes in the analyte concentration usually induce a change in the responsive electrical current, allowing for the establishment of a calibration plot between the target concentration and signal intensity [20,53,63], from which the analyte concentration can be determined by extrapolation by applying a mathematical algorithm. Based on the manner that the signal was collected in, diverse techniques such as cyclic voltammetry (CV) [42,75], amperometry [73,76], electrochemical impedance spectroscopy (EIS) [77,78], differential pulse voltammetry (DPV) [74,79], and square wave voltammetry (SWV) [80,81] were used. Amongst these, DPV, EIS, and SWV are considered to be better at improving sensitivity compared with CV and are widely applied for Aβ detection, which will be discussed in the next section.

3. Recent Research on Aβ Detection by Electrochemical Sensors

3.1. Electrochemical Sensors for Aβ Detection

Many studies have demonstrated that Aβ can be completely detected by employing an electrochemical sensor to obtain a low LOD at picograms or femtograms per milliliter [53,63,64,67,69–71,82]. The Aβ peptide structure has a tyrosine group, histidine, and methionine which participate in the redox reaction with an oxidized peak at ~0.6 and ~1.05 and wave at 1–1.5 V vs. Ag/AgCl on a carbon surface [83,84]. The oxidation occurring on the residual groups under a supplied voltage indicates the detection ability for Aβ biomarkers; however, this method detects a plethora of other proteins containing such groups as well. Non-specific adsorption during the detection of such proteins could be eliminated by designing an electrochemical immunosensor in which non-specific adsorption is prevented by blocking the residual surface with bovine serum albumin (BSA) [34,53,69].

The anti-Aβ antibody and Aβ antigen interaction taking place on the working electrode surface can be detected by diverse techniques such as CV [42], amperometry [73], DPV [63,64,69,70,72,85], EIS [53,62,65,71], and linear square voltammetry (LSV) [75]. Depending on the requirements, available equipment, and labor ability, each technique can be applied reasonably and effectively. Moreover, Aβ peptides can be detected using labels with enzymes, nanozymes, or anti-IgG-ALP, [86,87] or label-free using functional groups [88–90] in electrochemical detection methods.

3.2. Working Electrode Modification

The use of bare electrodes has shortcomings, such as low sensitivity, selectivity, and durability, which hamper the applicability of the Aβ electrochemical sensor due to a lack of an appropriate detection range and an inappropriate LOD, leading to it being less reliable and limiting the diagnostic application. To overcome these bottlenecks, many methods have been employed to modify the electrode surface, including designing different kinds of electrodes, synthesizing diversely structured nanomaterials, or amplifying the detectable signal. Among these, designing different kinds of electrodes requires expensive equipment along with skilled labor and amplifying the detectable signal is limited by a physical threshold, whereas diverse nanostructured materials on working electrodes have been intensively applied in laboratory environments employing metal, metal oxide, carbon, composite, conductive polymer, and SAM. Practically, tailoring the materials on

the electrode surface to achieve a better performance has been conducted in a variety of research areas, like energy [91,92], electrochemical sensors [61,63,93], etc. Electrode-modified electrochemical sensors prove their effectiveness by obtaining high sensitivity and selectivity [61,63,93], as illustrated in Figure 3. In this study, SAM-related content is focused on; however, to have an overview and enhance the logical comprehension of the present review, electrode modification based on the remaining kinds of materials is also discussed and outlined.

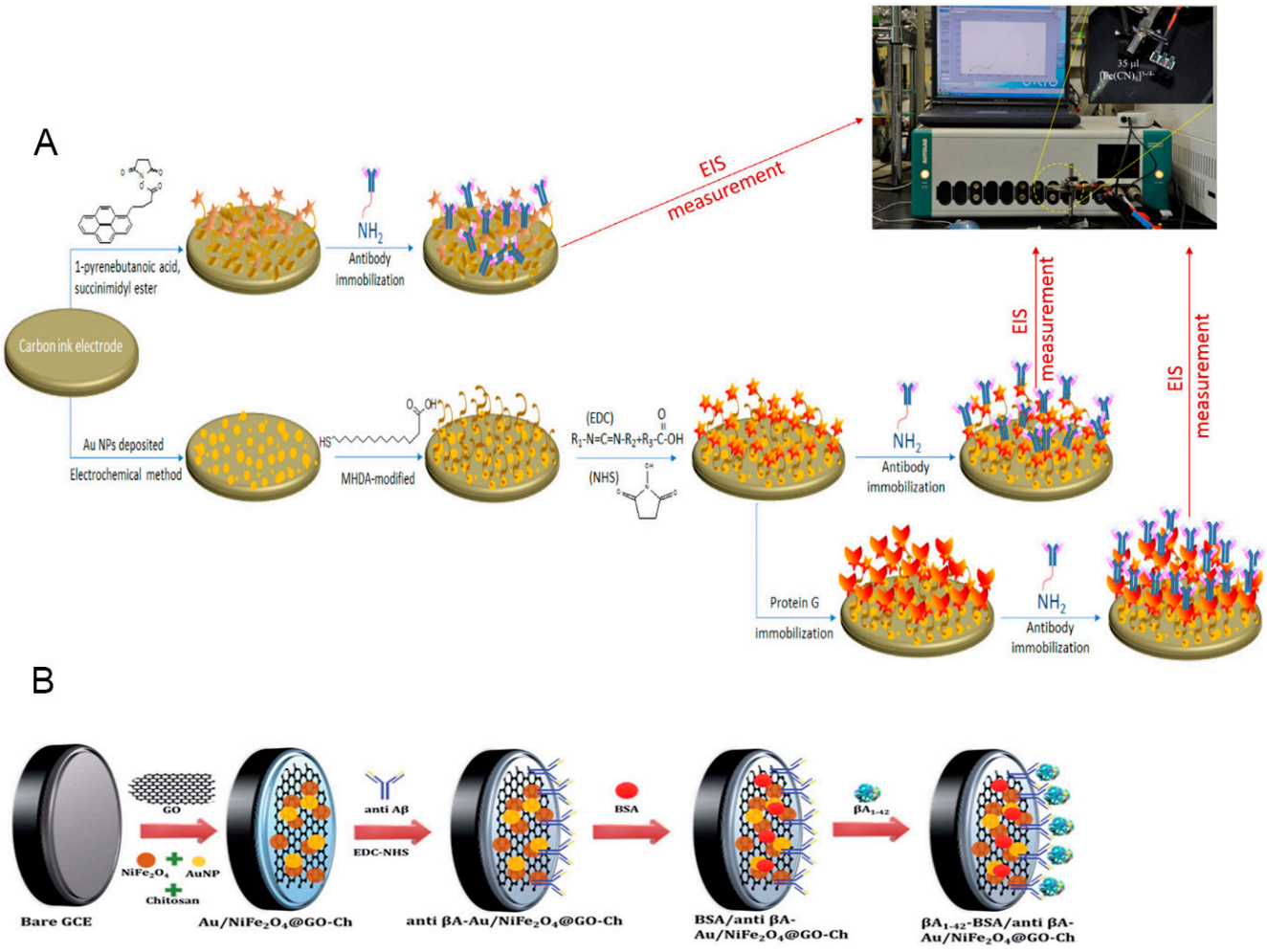

Figure 3. Tailoring the working electrode for the electrochemical biosensor. (**A**) The Au-based electrode was modified with an SAM, then orientation was assisted with protein G, and, finally, conjugated antibody Aβ [55]. (**B**) The bare GCE electrode was modified with Au and composite of $NiFe_2O_4$@GO-Ch, then we conjugated the antibody [65]. SAM, self-assembled monolayer.

3.2.1. Metal, Alloy, and Metal Oxide

The noble metal Au has been documented to enhance the Aβ peptide detective performance of electrochemical sensors. Dai et al. deposited a thin film of Au on the working and counter electrodes by vapor deposition on the atomic level [85]. The SAM used 3-Mercaptopropionic acid (MPA), then EDC and NHS were added for functionalization to conjugate antibody Aβ42. Aβ42 was detected using the DPV technique with 5 mM $[Fe(CN)_6]^{3-/4-}$ at various incubation times. The experiments were conducted in undiluted human serum at a linear range of 67.5–500 ng/mL. Lien et al. prepared a disposable electrochemical-printed (DEP) chip with Au deposition using CV techniques [62]. Then, antibodies were conjugated on the SAM layer to detect the Aβ peptides using the electrochemical impedance technique with 1–10^3 nM and an LOD of 2.65 nM. Further modification of the electrode with G protein increased the ability to detect Aβ(1-42) with a

linear range of 10 pM–100 nM and an LOD of 0.57 nM. Xia et al. reported an electrochemical immunosensor for the detection of Aβ oligomers (AβOs) [82], in which PrP(95-110) was labeled with adamantine (Ad) to form Ad-PrP(95-110), and then Ag nanoparticles (NPs) were add to a Ad-PrP(95-110) solution to form a mixture that was anchored onto a β-cyclodextrin (β-CD)-covered electrode surface through host–guest interaction; finally, the cyclodextrin-covered electrodes were incubated overnight with β-CD-SH and TCEP to link with the plate gold electrode, and the unreacted gold surface was blocked with the MCH solution. The fabricated sensor detected AβOs with a linear range of 20–100 nM and an LOD of 8 pM.

In addition to pure metal, alloy has also been used in electrochemical biosensors for detecting Aβ, as reported by Liu et al. [63]. They prepared an electrochemical aptasensor based on a combination of AuPt alloy nanoparticles and carbon fiber paper (CFP) to form CFP/AuPt which was then incubated with DNA aptamer to detect Aβ oligomers with a linear range of 0.5–10^4 pg/mL and an LOD of 0.16 pg/mL.

In addition, metal oxide has also been used for Aβ electrochemical sensors. Supraja et al. designed an electrochemical immunosensor relying on SnO_2 nanofibers (SNFs) [49]. SnO_2 metal oxide was drop-cast on the GCE surface and then functioned with -COOH to conjugate anti-AB42-antibody for immunoreaction. The fabricated sensor was able to detect β-amyloid(1-42) (AB42) with a linear range of 1 fg/mL to 10 ng/mL and an LOD of 0.146 fg/mL for AB42 spiked buffer, and linear range of 1 fg/mL to 1 ng/mL and an LOD of 0.638 fg/mL for plasma samples. The sensor can survive for over 126 days.

Metal oxide is inexpensive compared with novel metal and alloy, but it has proven to be effective in Aβ detection. Thus, the applicability of such materials in this kind of biosensor is immense.

3.2.2. Carbon-Based Materials

Carbon materials are famous for their high surface area, conductivity, and flexibility, which acts as a scaffold for tailoring or anchoring other elements in electrochemical biosensor applications. In addition, it contains many functional groups such as hydroxyl (-OH) and carboxyl (-COOH) which can be functionalized to conjugate antibodies for the antigen detection of Aβ. Sethi et al. designed a label-free electrochemical sensor based on the dual layer of graphene oxide and reduced graphene oxide to detect plasma-based $Aβ_{1-42}$ [64], which was modified with 1-pyrenebutyric acid N-hydroxysuccinimide ester (Pyr-NHS) to assist in H31L21 antibody immobilization. As a result, $Aβ_{1-40}$ was recognized with a linear range of 11–55 pM and an LOD of 2.398 pM. Chae et al. also constructed a carbon-based electrochemical sensor with the enhanced surface functionality of reduced graphene oxide (rGO) for diagnosing Alzheimer's disease [67]. GO was deposited on the substrate in 20 layers and was then treated with hydriodic acid (HI) to form a thin film of rGO, which was further treated to create a photo-resistant pattern, and finally lifted off; photolithography was then used to form the gold electrodes. The electrode was then incubated with EDC/NHS to immobilize 6E10 monoclonal antibody via covalent bonds with ethanolamine (ETA) to avoid any undesired covalent bonds. The oxygen-plasma-treated electrode exhibited a response 1.68-fold superior to that of the untreated electrodes in $Aβ_{42}$ detection. Ji et al. investigated the effect of various materials functionalized on graphene for Aβ detection [94] and recognized that the presence of Aβ on the surface of materials strongly affected electron transport. Hence, carbon-based materials are advantageous for fabricating electrochemical sensors for Aβ peptide detection.

3.2.3. Composite Materials

Composite materials are widely utilized for electrochemical sensors in general and for electrochemical biosensors in particular thanks to the synergetic effect between diverse materials to enhance the electrical signal and, therefore, improvement in the sensitivity and stability. Zhou et al. prepared an electrochemical aptasensor of Au-deposited vertical graphene/carbon cloth (VG/CC), and then cellular prion protein (PrPC) residues 95-110

were immobilized on the electrode surface based on the Au-S bond to Aβ oligomer [69]. Finally, poly(themine)-template Cu NPs were used as electrochemical probes for the aptasensor. The fabricated aptasensor detected Aβ with a linear range of 10–2200 pM and an LOD of 3.5 pM. In another report, Li et al. prepared bifunctional Pd-decorated Co_9S_8 polysulfide nanoparticles supported on graphene oxide (G/Co_9S_8-Pd) [71], which was deposited on the surface of GCE as a substrate for antibody conjugation by linking with Pd NPs after 1 h of incubation. The label-free electro immunosensor detected Aβ peptides with a linear range of 0.1 pg/mL–50 ng/mL and a low LOD of 41.4 pg/mL. Composite materials are promising candidates for electrochemical biosensor applications by improving the LOD toward higher sensitivity, which is a desired property for the design and practical application of biosensors.

3.2.4. Conductive Polymer

Conductive polymer with high electrical conductivity is also used for electrochemical sensors. In addition, functional groups on the structural surface facilitate the conjugation of antibodies for immunoreaction. Abbasi et al. prepared an electrochemical sensor with a conductive polymer with a controlled thickness on the screen-printed electrode [70]. Ultra-thin layers of polymerized 1,5-diaminonaphthalene (pDAN) were coated on the graphene layer of the electrode at a controlled thickness, and the anti-beta amyloid antibody was activated in a solution of EDC/NHS and conjugated on the conductive polymer; the free amine group was blocked by BSA. The sensor could detect $A\beta_{42}$ with a linear range of 1–1000 pg/mL, an LOD of 1.4 pg/mL, and a limit of quantification (LOQ) of 4.25 pg/mL. Zhao et al. prepared an electrochemical sensor with Au and PrP^c embedded in the conductive polymer matrix of poly(thiophene-3-acetic acid), poly(pyrrole-2-carboxylic acid), and poly (pyro-3-carboxylic acid) for the detection of AβO with a linear range of 10^{-9}–10^3 nM [95]. The PrP^c/AuNPs-E-Ppy-3-COOH-based sensor detected Aβ with an LOD of 10^{-9} nM. Conductive polymers with the advantageous features of high conductivity, flexibility, and structure-based functional groups are useful in electrochemical sensor applications.

3.2.5. SAM-Support-Based Working Electrodes for Aβ Electrochemical Sensors

Self-assembled monolayer (SAM) is ordered arrays of organic molecules and has been employed as monolayers on electrode surfaces in liquid or solid phases in many electronic devices, such as electrochemical sensors [4,34,96], batteries [54], solar cells [55], and organic field effect transistors (OFETs) [56], through SAM modification [57]. The working electrodes modified with SAM are depicted in Figure 4. The presence of an SAM on the working electrode structure acts as resistor, which contributes to the total impedance; thus, the study of SAM at a nanoscale level will help to tailor the chain length, create a defect-free electrode surface, and improve biosensor performance [97]. The layer orientation of the SAM tilts and twists at angles to the planar substrate surface, which varies with the material connected to the SAM; the presented atoms depend on the SAM composition with thickness-controlled layers [58]. A representative SAM structure consists of a head group (anchoring group), backbone (linkage), and tail group (functional group) [54–56]. The functionality of an SAM provides specific affinity to a substrate, while the alkanethiols on its structure enable adsorptability on the noble and coinage metals to form a high-order organic layer [98,99]. The thickness of an SAM is around 10 to 100 nm, and the deposition of an SAM on a metal surface can be performed by many techniques such as microcontact printing, scanning probes, and beams of photons, electrons, or atoms [4,34,57,58]. The SAM is deposited on a planar substrate that may be polycrystalline or single crystalline with a limited boundary [58]. Normally, Au- or Pd-based substrates are used for SAM [100,101] more frequently than other elements such as Ag-based substrates because of high conductivity, ease of bonding with the thiols group, avoidance of oxidation in the ambient environment, and nontoxicity to cells [102,103]. During SAM processing, ethanol has been used as a solvent because of its easy dissolution of alkanethiols, low cost, high purity, and low toxicity. The existence of terminally functional groups on the SAM surface allows for the

immobilization of antibodies, enzymes, DNA, polypeptides, and proteins [56]. The ion–pair interaction on the SAM surface is also strongly affected by the pH range [104]. Both single and mixed SAMs can be used in micro/nano electronic devices owing to tunable SAM configurations, enhancement of stability, and modulation of the rectification properties, improving device performance [59]. To conclude, research on the biocompatible surface of SAMs facilitates electron transfer between electrodes and localized immunoreaction that contributes to the improvement of electrochemical sensors.

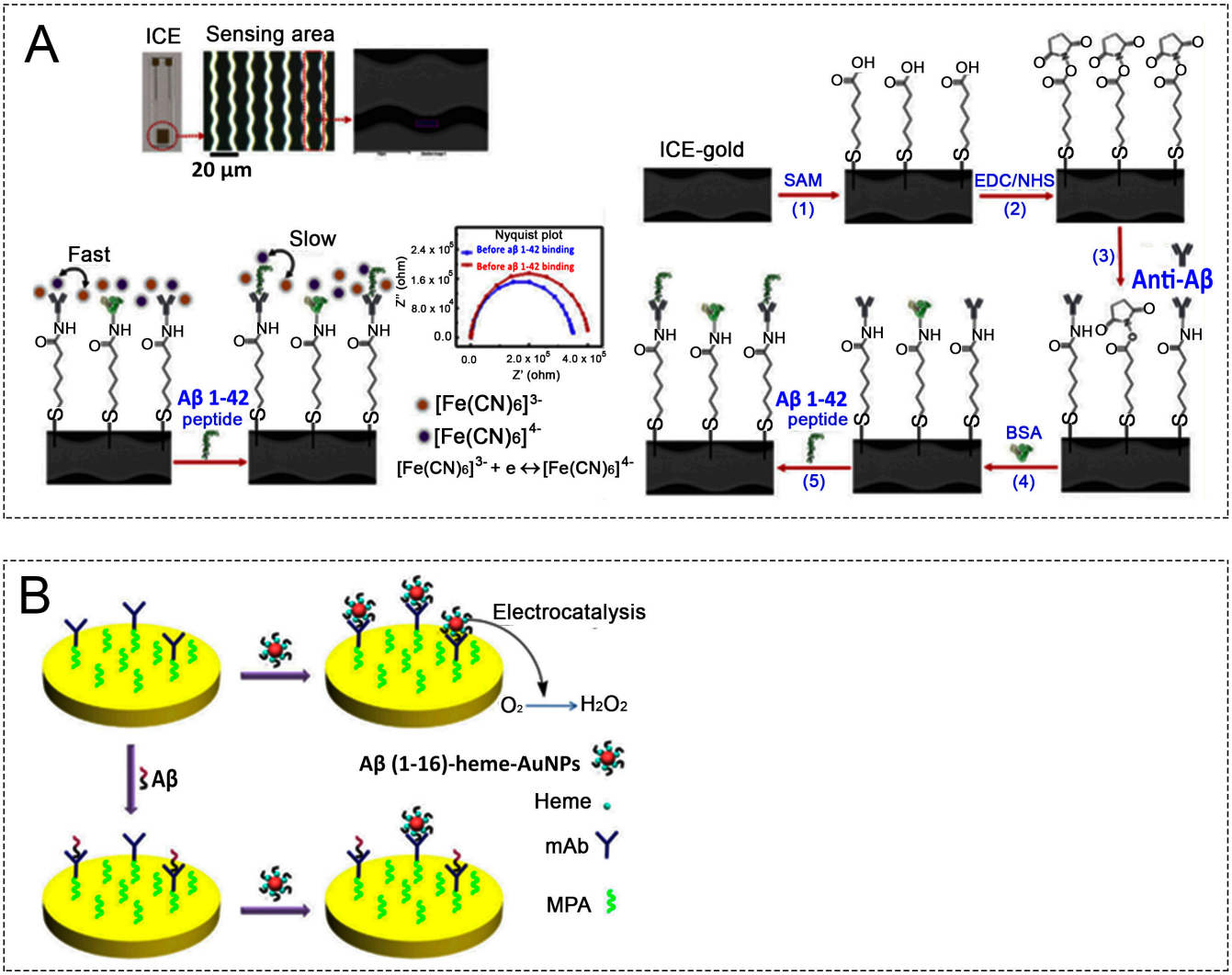

Figure 4. (**A**) Microscopic image of the sensing figures in ICE: Schematic of the biosensor construction at each stage of the process. The faradaic impedimetric surface engineering is based on the electron transfer resistance of the redox probe $[Fe(CN)6]^{3-/4-}$ in solution [4]. (**B**) Schematic representation of Aβ detection: Aβ(1-16) heme-Au NPs are attached onto the mAb-covered electrode without the Aβ capture step (**top**). A smaller number of Aβ(1-16)-heme-Au NPs are attached after incubation of the electrode with Aβ species (**bottom**) [38]. ICE, interdigitated chain-shaped electrode; NPs, nanoparticles.

SAM construction on the working electrode can be carried out by diverse organic compounds, including organosulfur [58,105], organosilanes [105], phosphates [106], and carboxylic acid [105,107]. Each of them required a type of substrate corresponding to head group structure. In the organosulfur case, thanks to the sulfur-containing group, Au-S chemical bonding formation can be easily achieved, facilitating this for the head group of alkanethiols anchoring on the Au surface by reductive elimination of the hydrogen.

The bonding energy of the Au-S was estimated to be roughly 40 kcal·mol^{-1} [54,56,92]. Organosulfur-compounds-based SAM in electrochemical sensors has been employed for Aβ peptides detection [4,42,53,85]. In the case of organosilanes, silanol of the organic precursor can attach to hydroxylated surfaces, for example, silicon oxide (SiO_2), alumina, glass, zinc oxide (ZnO), indium oxide (In_2O_3), mica, and germanium dioxide (GeO_2) [56,105]. Generally, hydroxyl group is not available on such kinds of surfaces; therefore, the substrates should be treated by utilizing piranha solution or oxygen plasma to obtain required surfaces [56]. Generation of the -OH group after treatment makes the substrates hydrophilic, promoting the formation of a highly ordered monolayer. Compared to organosilanes and organosulfur compounds, which have been utilized frequently in fabricating SAM, whereas an insignificant amount of carboxylic-acid- and phosphate-based SAM was also studied on metal oxide substrates [105,107]. Based on the above analyses, the selection of SAM organic precursor strongly depends on the kinds of utilized substrates. Furthermore, SAM length, SAM concentration, SAM moiety, temperature, and incubation time decide the quality of the produced SAM, which therefore directly impacts SAM impedance. What is more, the type of moieties and their distribution determine the number of immobilized antibodies or enzymes, and these accompany biochemical reaction efficiency as well as sensor performance.

SAMs have been applied in electrochemical biosensors for the detection of Aβ peptides, an Alzheimer's biomarker. Among several abovementioned precursors for SAM formation, the application of organosulfur in manufacturing Aβ electrochemical sensor is predominant, in which pristine Au electrode has been linked with thiol-groups. Indeed, Hien et al. used an interdigitated chain-shaped electrode with an Au surface [4]: 6-mercaptohexanoic acid (MHA) was attached to the surface to form an SAM and activated with EDC/NHS to prepare for anti-Aβ antibody conjugation. The fabricated sensor enabled the detection of $Aβ_{1-42}$ with a linear range of 10^{-3}–10^{3} ng/mL and a low LOD of 100 pg/mL in HS and approximately 500 pg/mL in CSF. Liu et al. prepared an SAM by incubating the cleaned gold electrode with MPA in the dark for 12 h and then activated the SAM with EDC/NHSS to conjugate antibody by cross-linking [42]. In addition, Aβ(1-16)-heme-AuNP was generated by a ligand exchange reaction between Aβ(1-16)Cys and citrate-stabilized AuNPs. Aβ(1-16) and Aβ(1-16)-heme-AuNPs were detected by casting on the mAb-covered electrode for 10 min and using the voltametric technique in an air-saturated solution. Aβ detection was performed in a spiked sample with an Aβ(1-40)/Aβ(1-42) ratio of 6:1, similar to the real ratio in the CSF, resulting in a linear range of 0.02–1.50 nM with an LOD of 10 pM. Similarly, Dai et al. fabricated an SAM on the Au surface to conjugate antibodies for β-amyloid 42 detection. The sensor detected Aβ with a linear range of 0.0675–0.5 µg/mL [85]. Supraja et al. prepared an electrochemical immunosensor with an SAM made from MPA for detecting Aβ with a detection range of 1 fg/mL–1 ng/mL and an LOD of 0.146 fg/mL and 0.638 fg/mL in spiked buffer and plasma samples, respectively, as presented above [49]. Compared to the organosulfur-precursor-related publication, SAM formation based on organosilanes, carboxylic acid, and phosphates precursors for Aβ electrochemical sensors is very limited.

SAMs on electrochemical biosensor electrodes enable the conjugation of the antibody, which proves the immunosensor's ability to detect the Aβ biomarker with a low LOD. Basically, SAM preparation is a type of electrode modification, and selecting the appropriate SAM with thickness-controlled layers can increase sensitivity, and therefore improve the LOD, an important factor for electrochemical biosensors in biomedical applications. All studies discussed in the present review are tabulated in Table 1.

Table 1. Studies of Aβ detection using electrochemical biosensors.

No.	Material	Analyte	Bio-Fluids	Detection Technique	Linear Range	LOD	Ref.
1	Au/SAM/NHS-EDC/Ab-Aβ42	Aβ(1-42)	Undiluted HR (*)	DPV	0.0675–0.5 g/mL	NA (**)	[78]
2	-DEP/Au/MHDA-EDC/Ab-Aβ -DEP/Au/MHDA-EDC/protein G/Ab-Aβ	Aβ(1-40) Aβ(1-40)	PBS PBS	EIS EIS	1 to 10^3 nM 10 to 10^5 pM	2.65 nM 0.57 nM	[55]
3	CFP/AuPt/DNA aptamer	AβO	HS	DPV	0.5 to 10^4 pg/mL	0.16 pg/mL	[56]
4	β-CD modified Au electrode/MCH/Ad-Pr(95-110)/Ag	AβOs	PBS	LSV	20 to 10^5 pM	8 pM	[75]
5	GCE/SNF/(EDC-NHS)/Aβ42 antibodies/BSA	Aβ(1-42) Aβ(1-42)	Spiked sample Plasma	EIS	1 to 10^7 fg/mL 1 to 10^6 fg/mL	0.146 fg/mL 0.638 fg/mL	[49]
6	rGO/Pyr-NHS/H31L21/Ab-Aβ/BSA	Aβ(1-42)	Human blood	DPV	11 to 55.10^3 pM	2.398 pM	[57]
7	$NiFe_2O_4$ decorated GO/Au/Ab-Aβ/BSA	Aβ(1-42)	PBS	DPV	1 to 10^3 mg/mL	3.0 pg/mL	[65]
8	G/Co_9S_8-Pd/Ab-Aβ/BSA	Aβ	Spiked CSF	Amperometry	0.1 to 50.10^3 pg/mL	41.4 fg/mL	[64]
9	Au-VG/CC/PrP^c/Aptamer-poly T-CuNPs	Aβ oligomer	PB	DPV	10 to 2200 pM	3.5 pM	[62]
10	SPGE/pDAN/Ab-Aβ/BSA	Aβ(1-42)	Spiked plasma	DPV	1 to 1000 pg/mL	1.4 pg/mL	[63]
11	PrP^c/AuNPs-E-PTAA PrP^c/AuNPs-E-Ppy-2-COOH PrP^c/AuNPs-E-Ppy-3-COOH	AβO	CSF	EIS	10^{-9} to 10^3 nM 10^{-9} to 10^3 nM 10^{-9} to 10^3 nM	NA NA 10^{-9} nM	[88]
12	BSA/CGG CGG Chit/CCG DA/CCG DNA/CCG Gel/CCG PEG/CCG	Aβ40 Aβ42	CSF	EIS	NA	NA	[87]

(*) HR: human serum. (**) NA: not available.

4. Conclusions and Future Perspectives

This review presented electrochemical sensors for detecting a biomarker of Alzheimer's disease with a discussion of material modification for the working electrode which exhibits promising ability in the detection of the Aβ biomarker in human serum, blood, saliva, and CSF at a low LOD of picomoles to femtomoles per liter. Especially, the use of SAMs improved the electrode surface, which is a conjunction between the antibody and pristine electrode. SAM demonstrated advantages in antibody conjugation, improved orientation, and conjunction bridge for electron transfer. However, SAM still has some drawbacks, such as the time-consuming process, difficulty in uniformly controlling SAM, and defect formation during processing.

To surmount these obstacles, research on SAM design for electrochemical sensors requires progress in the following areas:

1. Screening the organic substance for SAM formation to precisely tailor the surface properties down to the nanoscale. Relying on a specific purpose, SAM can be prepared on various substrates, e.g., silicon, Au, and metal oxide; therefore, the type of organic precursors should be chosen appropriately, then other factors, namely chain length and functional group, also should be considered for optimization.
2. Reducing time processing by avoiding the activated step without utilizing the NHS/EDC. In aforementioned works, the functional groups must have been activated by NHS/EDC to graft suitably functional groups serving for antibody immobilization. Such work consumes time and makes progression complicated. Thus, utilization of the precursor with desired functional groups can shorten the processing time.
3. Controlling the thickness of the layer by employing cutting-edge technologies. The design and fabrication of SAM on the working electrode surface can be performed by various methods, for instance, micro contact printing, scanning probe lithography, and photo-induced pattering. Each method generates its own SAM thickness, which

significantly affects the electron transfer ability. Hence, for a specific organic precursor, the construction of SAM by employing the cantilever can contract SAM thickness compared to other method counterparts. However, the EFM machine is too pricey and must be operated by skilled operators.

4. The reasonable design of defect-free SAMs and study at the molecular scale to enhance sensor performance. SAM construction on the specific surface usually produces structural defects, causing a reduction in the electrochemical sensor performance. Thus, the study of SAM formation at the nanoscale can make the structural defects controllable.

Author Contributions: Conceptualization, writing—original draft preparation, P.G.L.; methodology, P.G.L.; validation, H.T.N.L. and H.-E.K.; writing—review and editing, supervision, S.C. All authors have read and agreed to the published version of the manuscript.

Funding: This work was supported by the National Research Foundation of Korea (NRF) grant funded by the Korea government (MSIT) (No.2022R1F1A1064357), and the Gachon University research fund of 2020 (GCU-2020-02710001).

Institutional Review Board Statement: Not applicable.

Informed Consent Statement: Not applicable.

Data Availability Statement: Not applicable.

Conflicts of Interest: The authors declare no conflict of interest.

References

1. Jiang, M.; Wang, X.-Y.; Wang, X.-B. Advances in Detection Methods of β-Amyloid Protein. *Chin. J. Anal. Chem.* **2018**, *46*, 1339–1349. [CrossRef]
2. Breijyeh, Z.; Karaman, R. Comprehensive Review on Alzheimer's Disease: Causes and Treatment. *Molecules* **2020**, *25*, 5789. [CrossRef] [PubMed]
3. Wang, B.-Y.; Gu, B.-C.; Wang, G.-J.; Yang, Y.-H.; Wu, C.-C. Detection of Amyloid-β(1-42) Aggregation with a Nanostructured Electrochemical Sandwich Immunoassay Biosensor. *Front. Bioeng. Biotechnol.* **2022**, *10*, 853947. [CrossRef] [PubMed]
4. Ngoc Le, H.T.; Park, J.; Chinnadayyala, S.R.; Cho, S. Sensitive electrochemical detection of amyloid beta peptide in human serum using an interdigitated chain-shaped electrode. *Biosens. Bioelectron.* **2019**, *144*, 111694. [CrossRef]
5. Jamerlan, A.; An, S.S.A.; Hulme, J. Advances in amyloid beta oligomer detection applications in Alzheimer's disease. *TrAC Trends Anal. Chem.* **2020**, *129*, 115919. [CrossRef]
6. Chen, J.; Lin, K.-C.; Prasad, S.; Schmidtke, D.W. Label free impedance based acetylcholinesterase enzymatic biosensors for the detection of acetylcholine. *Biosens. Bioelectron.* **2023**, *235*, 115340. [CrossRef]
7. Deshwal, A.; Gill, A.K.; Nain, S.; Patra, D.; Maiti, S. Inhibitory effect of nucleotides on acetylcholine esterase activity and its microflow-based actuation in blood plasma. *Chem. Commun.* **2022**, *58*, 3501–3504. [CrossRef] [PubMed]
8. Gu, X.; Wang, X. An overview of recent analysis and detection of acetylcholine. *Anal. Biochem.* **2021**, *632*, 114381. [CrossRef]
9. Zhang, Y.; Ding, L.; Zhang, H.; Wang, P.; Li, H. A new optical fiber biosensor for acetylcholine detection based on pH sensitive fluorescent carbon quantum dots. *Sens. Actuators B Chem.* **2022**, *369*, 132268. [CrossRef]
10. Chen, G.-F.; Xu, T.-H.; Yan, Y.; Zhou, Y.-R.; Jiang, Y.; Melcher, K.; Xu, H.E. Amyloid beta: Structure, biology and structure-based therapeutic development. *Acta Pharmacol. Sin.* **2017**, *38*, 1205–1235. [CrossRef]
11. Thal, D.R.; Beach, T.G.; Zanette, M.; Heurling, K.; Chakrabarty, A.; Ismail, A.; Smith, A.P.L.; Buckley, C. [18F]flutemetamol amyloid positron emission tomography in preclinical and symptomatic Alzheimer's disease: Specific detection of advanced phases of amyloid-β pathology. *Alzheimer's Dement.* **2015**, *11*, 975–985. [CrossRef] [PubMed]
12. Sundgren-Andersson, A.K.; Svensson, S.P.S.; Swahn, B.-M.; Juréus, A.; Sandell, J.; Johnson, A.E.; Jeppsson, F.; Neelissen, J.A.M.; Halldin, C.; Johnström, P.; et al. AZD4694: Fluorinated Positron Emission Tomography (PET) radioligand for detection of β-amyloid deposits. *Alzheimer's Dement.* **2009**, *5*, 57. [CrossRef]
13. Geraldes, C.F.G.C.; Lacerda, S.; Tóth, É. Molecular Probes for Magnetic Resonance Imaging of Amyloid β Peptides. In *Reference Module in Chemistry, Molecular Sciences and Chemical Engineering*; Elsevier: Amsterdam, The Netherlands, 2018. [CrossRef]
14. Yanagisawa, D.; Amatsubo, T.; Morikawa, S.; Taguchi, H.; Urushitani, M.; Shirai, N.; Hirao, K.; Shiino, A.; Inubushi, T.; Tooyama, I. In vivo detection of amyloid β deposition using 19F magnetic resonance imaging with a 19F-containing curcumin derivative in a mouse model of Alzheimer's disease. *Neuroscience* **2011**, *184*, 120–127. [CrossRef]
15. Allsop, D.; Swanson, L.; Moore, S.; Davies, Y.; El Agnaf, O.; Soutar, I. Sensitive detection of β-amyloid aggregation by means of time-resolved fluorescence polarisation anisotropy. *Neurobiol. Aging* **2000**, *21*, 20–21. [CrossRef]

16. Chen, X.; Li, Y.; Kang, J.; Ye, T.; Yang, Z.; Liu, Z.; Liu, Q.; Zhao, Y.; Liu, G.; Pan, J. Application of a novel coumarin-derivative near-infrared fluorescence probe to amyloid-β imaging and inhibition in Alzheimer's disease. *J. Lumin.* **2023**, *256*, 119661. [CrossRef]
17. Wang, Z.; Jiao, Y.; Ding, Q.; Song, Y.; Ma, Q.; Ren, H.; Lu, K.; Jia, S.; Cui, J. A bioinspired fluorescent probe based on metal–organic frameworks to selectively enrich and detect amyloid-β peptide. *Chem. Eng. J.* **2023**, *470*, 144124. [CrossRef]
18. Yue, N.; Fu, H.; Chen, Y.; Gao, X.; Dai, J.; Cui, M. Rational design of molecular rotor-based fluorescent probes with bi-aromatic rings for efficient in vivo detection of amyloid-β plaques in Alzheimer's disease. *Eur. J. Med. Chem.* **2022**, *243*, 114715. [CrossRef]
19. Zhuo, C.; Li, Z.; Cui, J.; Song, Z.; Tang, Q.; Yin, Y.; Zhang, G.; Liao, X.; Liu, Z.; Gao, F. DNAzyme-driven bipedal DNA walker triggered to hybridize silver nanoparticle probes for electrochemical detection of amyloid-β oligomer. *Anal. Chim. Acta* **2023**, *1246*, 340889. [CrossRef] [PubMed]
20. Zhang, B.; Zhu, T.; Liu, L.; Yuan, L. In vitro electrochemical detection of the degradation of amyloid-β oligomers. *J. Colloid Interface Sci.* **2023**, *629*, 156–165. [CrossRef] [PubMed]
21. Liao, X.; Zhang, C.; Shi, Z.; Shi, H.; Qian, Y.; Gao, F. Signal-on and label-free electrochemical detection of amyloid β oligomers based on dual amplification induced hemin/G-quadruplex formation. *J. Electroanal. Chem.* **2020**, *878*, 114604. [CrossRef]
22. Yan, J.; Wen, X.; Yin, L.; Wang, Y.; Li, H.; Tu, Y. An electrochemiluminescence aptasensor for amyloid-β protein with signal enhancement from AuNPs/Fe-MOFs nanocomposite. *J. Electroanal. Chem.* **2023**, *933*, 117293. [CrossRef]
23. Zhang, N.; Liu, S.; Jia, Y.; Zhao, G.; Duan, X.; Wang, Y.; Zhang, D.; Wei, Q. Ultrasensitive electrochemiluminescence immunosensor based on Co-doped MoOx as co-reactant generator for the detection of amyloid β-protein. *Microchem. J.* **2022**, *183*, 108036. [CrossRef]
24. Meng, S.; Qin, D.; Wu, Y.; Mo, G.; Jiang, X.; Deng, B. Electrochemiluminescence resonance energy transfer of MnCO3 for ultrasensitive amyloid-β protein detection. *Talanta* **2023**, *253*, 123993. [CrossRef] [PubMed]
25. Guo, Q.; Yang, J.; Zhao, J.; Zhang, J.; Yuan, R.; Chen, S. A novel aptamer biosensor based on polydopamine quenched electrochemiluminescence of polyfluorene nanoparticles for amyloid-β oligomers detection. *Sens. Actuators B Chem.* **2022**, *368*, 132204. [CrossRef]
26. Jandas, P.J.; Prabakaran, K.; Luo, J.; Derry, H.M.G. Effective utilization of quartz crystal microbalance as a tool for biosensing applications. *Sens. Actuators A Phys.* **2021**, *331*, 113020. [CrossRef]
27. Wang, C.; Liu, M.; Zhang, D.; Li, P.; Wang, D.; Sun, S.; Wei, W. Detection of β-amyloid peptide aggregates by quartz crystal microbalance based on dual-aptamer assisted signal amplification. *Anal. Chim. Acta* **2023**, *1244*, 340857. [CrossRef]
28. Hwang, S.S.; Chan, H.; Sorci, M.; Van Deventer, J.; Wittrup, D.; Belfort, G.; Walt, D. Detection of amyloid β oligomers toward early diagnosis of Alzheimer's disease. *Anal. Biochem.* **2019**, *566*, 40–45. [CrossRef]
29. Dickerson, B.C.; Bakkour, A.; Salat, D.H.; Feczko, E.; Pacheco, J.; Greve, D.N.; Grodstein, F.; Wright, C.I.; Blacker, D.; Rosas, H.D.; et al. The Cortical Signature of Alzheimer's Disease: Regionally Specific Cortical Thinning Relates to Symptom Severity in Very Mild to Mild AD Dementia and is Detectable in Asymptomatic Amyloid-Positive Individuals. *Cereb. Cortex* **2009**, *19*, 497–510. [CrossRef]
30. Guo, Y.; Leng, H.; Chen, Q.; Su, J.; Shi, W.-j.; Xia, C.; Zhang, L.; Yan, J. Development of novel near-infrared GFP chromophore-based fluorescent probes for imaging of amyloid-β plaque and viscosity. *Sens. Actuators B Chem.* **2022**, *372*, 132648. [CrossRef]
31. Park, Y.D.; Kinger, M.; Min, C.; Lee, S.Y.; Byun, Y.; Park, J.W.; Jeon, J. Synthesis and evaluation of curcumin-based near-infrared fluorescent probes for the in vivo optical imaging of amyloid-β plaques. *Bioorgan. Chem.* **2021**, *115*, 105167. [CrossRef] [PubMed]
32. Bullich, S.; Seibyl, J.; Catafau, A.M.; Jovalekic, A.; Koglin, N.; Barthel, H.; Sabri, O.; De Santi, S. Optimized classification of 18F-Florbetaben PET scans as positive and negative using an SUVR quantitative approach and comparison to visual assessment. *NeuroImage Clin.* **2017**, *15*, 325–332. [CrossRef] [PubMed]
33. Morris, E.; Chalkidou, A.; Hammers, A.; Peacock, J.; Summers, J.; Keevil, S. Diagnostic accuracy of 18F amyloid PET tracers for the diagnosis of Alzheimer's disease: A systematic review and meta-analysis. *Eur. J. Nucl. Med. Mol. Imaging* **2016**, *43*, 374–385. [CrossRef] [PubMed]
34. Le, H.T.N.; Kim, D.; Phan, L.M.T.; Cho, S. Ultrasensitive capacitance sensor to detect amyloid-beta 1-40 in human serum using supramolecular recognition of β-CD/RGO/ITO micro-disk electrode. *Talanta* **2022**, *237*, 122907. [CrossRef] [PubMed]
35. Tu, Y.; Wu, J.; Chai, K.; Hu, X.; Hu, Y.; Shi, S.; Yao, T. A turn-on unlabeled colorimetric biosensor based on aptamer-AuNPs conjugates for amyloid-β oligomer detection. *Talanta* **2023**, *260*, 124649. [CrossRef]
36. Devi, R.; Gogoi, S.; Dutta, H.S.; Saikia, P.J.; Singhal, A.; Khan, R. Boronic acid-functionalized tungsten disulfide quantum dots as a fluorescence probe for sensitive detection of dopamine. *Biosens. Bioelectron. X* **2022**, *11*, 100168. [CrossRef]
37. Nguyen, Q.H.; Lee, D.H.; Nguyen, P.T.; Le, P.G.; Kim, M.I. Foldable paper microfluidic device based on single iron site-containing hydrogel nanozyme for efficient glucose biosensing. *Chem. Eng. J.* **2023**, *454*, 140541. [CrossRef]
38. Liu, X.; Li, X.; Xu, S.; Guo, S.; Xue, Q.; Wang, H. Efficient ratiometric fluorescence probe based on dual-emission luminescent lanthanide coordination polymer for amyloid β-peptide detection. *Sens. Actuators B Chem.* **2022**, *352*, 131052. [CrossRef]
39. Tan, S.; Li, S.; Tang, C.; Bai, X.; Ran, X.; Qu, Q.; Li, L.; Yang, L. A regenerable and reducing false-positive fluorescent switch for detection of β-amyloid 1-42 oligomers. *Talanta* **2022**, *246*, 123461. [CrossRef] [PubMed]
40. Kaur, H.; Siwal, S.S.; Saini, R.V.; Singh, N.; Thakur, V.K. Significance of an Electrochemical Sensor and Nanocomposites: Toward the Electrocatalytic Detection of Neurotransmitters and Their Importance within the Physiological System. *ACS Nanosci. Au* **2023**, *3*, 1–27. [CrossRef]

41. Ranjan, P.; Khan, R. Electrochemical Immunosensor for Early Detection of β-Amyloid Alzheimer's Disease Biomarker Based on Aligned Carbon Nanotubes Gold Nanocomposites. *Biosensors* **2022**, *12*, 1059. [CrossRef] [PubMed]
42. Liu, L.; Zhao, F.; Ma, F.; Zhang, L.; Yang, S.; Xia, N. Electrochemical detection of β-amyloid peptides on electrode covered with N-terminus-specific antibody based on electrocatalytic O_2 reduction by Aβ(1-16)-heme-modified gold nanoparticles. *Biosens. Bioelectron.* **2013**, *49*, 231–235. [CrossRef] [PubMed]
43. Gai, Z.; Li, F.; Yang, X. Electrochemiluinescence monitoring the interaction between human serum albumin and amyloid-β peptide. *Bioelectrochemistry* **2023**, *149*, 108315. [CrossRef]
44. Liu, W.; Zhang, H.; Dong, X.; Sun, Y. Composite of gold nanoclusters and basified human serum albumin significantly boosts the inhibition of Alzheimer's β-amyloid by photo-oxygenation. *Acta Biomater.* **2022**, *144*, 157–167. [CrossRef] [PubMed]
45. Ashton, N.J.; Blennow, K.; Zetterberg, H. Spitting image: Can saliva biomarkers reflect Alzheimer's disease? *EBioMedicine* **2021**, *68*, 103437. [CrossRef] [PubMed]
46. Reale, M.; Gonzales-Portillo, I.; Borlongan, C.V. Saliva, an easily accessible fluid as diagnostic tool and potent stem cell source for Alzheimer's Disease: Present and future applications. *Brain Res.* **2020**, *1727*, 146535. [CrossRef] [PubMed]
47. Tachida, Y.; Miura, S.; Muto, Y.; Takuwa, H.; Sahara, N.; Shindo, A.; Matsuba, Y.; Saito, T.; Taniguchi, N.; Kawaguchi, Y.; et al. Endothelial expression of human amyloid precursor protein leads to amyloid β in the blood and induces cerebral amyloid angiopathy in knock-in mice. *J. Biol. Chem.* **2022**, *298*, 101880. [CrossRef]
48. Kotiya, D.; Leibold, N.; Verma, N.; Jicha, G.A.; Goldstein, L.B.; Despa, F. Rapid, scalable assay of amylin-β amyloid co-aggregation in brain tissue and blood. *J. Biol. Chem.* **2023**, *299*, 104682. [CrossRef]
49. Crosnier de Lassichère, C.; Duc Mai, T.; Taverna, M. Antibody-free detection of amyloid beta peptides biomarkers in cerebrospinal fluid using capillary isotachophoresis coupled with mass spectrometry. *J. Chromatogr. A* **2019**, *1601*, 350–356. [CrossRef]
50. Chen, M.; Man, Y.; Xu, S.; Wu, H.; Ling, P.; Gao, F. A label-free dually-amplified aptamer sensor for the specific detection of amyloid-beta peptide oligomers in cerebrospinal fluids. *Anal. Chim. Acta* **2023**, *1266*, 341298. [CrossRef]
51. Supraja, P.; Tripathy, S.; Singh, R.; Singh, V.; Chaudhury, G.; Singh, S.G. Towards point-of-care diagnosis of Alzheimer's disease: Multi-analyte based portable chemiresistive platform for simultaneous detection of β-amyloid (1-40) and (1-42) in plasma. *Biosens. Bioelectron.* **2021**, *186*, 113294. [CrossRef]
52. Sharma, P.K.; Kim, E.-S.; Mishra, S.; Ganbold, E.; Seong, R.-S.; Kim, Y.M.; Jahng, G.-H.; Rhee, H.Y.; Han, H.-S.; Kim, D.H.; et al. Ultrasensitive probeless capacitive biosensor for amyloid beta (Aβ1-42) detection in human plasma using interdigitated electrodes. *Biosens. Bioelectron.* **2022**, *212*, 114365. [CrossRef] [PubMed]
53. Supraja, P.; Tripathy, S.; Vanjari, S.R.K.; Singh, R.; Singh, V.; Singh, S.G. Label-free detection of β-Amyloid (1-42) in plasma using electrospun SnO_2 nanofiber based electro-analytical sensor. *Sens. Actuators B Chem.* **2021**, *346*, 130522. [CrossRef]
54. Yi, R.; Mao, Y.; Shen, Y.; Chen, L. Self-Assembled Monolayers for Batteries. *J. Am. Chem. Soc.* **2021**, *143*, 12897–12912. [CrossRef] [PubMed]
55. Ali, F.; Roldán-Carmona, C.; Sohail, M.; Nazeeruddin, M.K. Applications of Self-Assembled Monolayers for Perovskite Solar Cells Interface Engineering to Address Efficiency and Stability. *Adv. Energy Mater.* **2020**, *10*, 2002989. [CrossRef]
56. Singh, M.; Kaur, N.; Comini, E. The role of self-assembled monolayers in electronic devices. *J. Mater. Chem. C* **2020**, *8*, 3938–3955. [CrossRef]
57. Le, H.T.N.; Phan, L.M.T.; Cho, S. Removal of Thiol-SAM on a Gold Surface for Re-Use of an Interdigitated Chain-Shaped Electrode. *Materials* **2022**, *15*, 2218. [CrossRef]
58. Love, J.C.; Estroff, L.A.; Kriebel, J.K.; Nuzzo, R.G.; Whitesides, G.M. Self-Assembled Monolayers of Thiolates on Metals as a Form of Nanotechnology. *Chem. Rev.* **2005**, *105*, 1103–1170. [CrossRef]
59. Khalid, H.; Opodi, E.M.; Song, X.; Wang, Z.; Li, B.; Tian, L.; Yu, X.; Hu, W. Modulated Structure and Rectification Properties of a Molecular Junction by a Mixed Self-Assembled Monolayer. *Langmuir* **2022**, *38*, 10893–10901. [CrossRef]
60. Vestergaard, M.d.; Kerman, K.; Saito, M.; Nagatani, N.; Takamura, Y.; Tamiya, E. A Rapid Label-Free Electrochemical Detection and Kinetic Study of Alzheimer's Amyloid Beta Aggregation. *J. Am. Chem. Soc.* **2005**, *127*, 11892–11893. [CrossRef] [PubMed]
61. Ye, M.; Jiang, M.; Cheng, J.; Li, X.; Liu, Z.; Zhang, W.; Mugo, S.M.; Jaffrezic-Renault, N.; Guo, Z. Single-layer exfoliated reduced graphene oxide-antibody Tau sensor for detection in human serum. *Sens. Actuators B Chem.* **2020**, *308*, 127692. [CrossRef]
62. Lien, T.T.N.; Takamura, Y.; Tamiya, E.; Vestergaard, M.d.C. Modified screen printed electrode for development of a highly sensitive label-free impedimetric immunosensor to detect amyloid beta peptides. *Anal. Chim. Acta* **2015**, *892*, 69–76. [CrossRef] [PubMed]
63. Liu, Y.; Xu, Q.; Zhang, Y.; Ren, B.; Huang, L.; Cai, H.; Xu, T.; Liu, Q.; Zhang, X. An electrochemical aptasensor based on AuPt alloy nanoparticles for ultrasensitive detection of amyloid-β oligomers. *Talanta* **2021**, *231*, 122360. [CrossRef] [PubMed]
64. Sethi, J.; Van Bulck, M.; Suhail, A.; Safarzadeh, M.; Perez-Castillo, A.; Pan, G. A label-free biosensor based on graphene and reduced graphene oxide dual-layer for electrochemical determination of beta-amyloid biomarkers. *Microchim. Acta* **2020**, *187*, 288. [CrossRef] [PubMed]
65. Qin, J.; Park, J.S.; Jo, D.G.; Cho, M.; Lee, Y. Curcumin-based electrochemical sensor of amyloid-β oligomer for the early detection of Alzheimer's disease. *Sens. Actuators B Chem.* **2018**, *273*, 1593–1599. [CrossRef]
66. Yoo, Y.K.; Kim, G.; Park, D.; Kim, J.; Kim, Y.; Yun Kim, H.; Yang, S.H.; Lee, J.H.; Hwang, K.S. Gold nanoparticles assisted sensitivity improvement of interdigitated microelectrodes biosensor for amyloid-β detection in plasma sample. *Sens. Actuators B Chem.* **2020**, *308*, 127710. [CrossRef]

67. Chae, M.-S.; Kim, J.; Jeong, D.; Kim, Y.; Roh, J.H.; Lee, S.M.; Heo, Y.; Kang, J.Y.; Lee, J.H.; Yoon, D.S.; et al. Enhancing surface functionality of reduced graphene oxide biosensors by oxygen plasma treatment for Alzheimer's disease diagnosis. *Biosens. Bioelectron.* **2017**, *92*, 610–617. [CrossRef] [PubMed]
68. Fan, K.; Yang, R.; Zhao, Y.; Zang, C.; Miao, X.; Qu, B.; Lu, L. A fluorescent aptasensor for sensitive detection of isocarbophos based on AT-rich three-way junctions DNA templated copper nanoparticles and Fe_3O_4@GO. *Sens. Actuators B Chem.* **2020**, *321*, 128515. [CrossRef]
69. Zhou, Y.; Lv, Y.; Dong, H.; Liu, L.; Mao, G.; Zhang, Y.; Xu, M. Ultrasensitive assay of amyloid-beta oligomers using Au-vertical graphene/carbon cloth electrode based on poly(thymine)-templated copper nanoparticles as probes. *Sens. Actuators B Chem.* **2021**, *331*, 129429. [CrossRef]
70. Abbasi, H.Y.; Tehrani, Z.; Devadoss, A.; Ali, M.M.; Moradi-Bachiller, S.; Albani, D.; Guy, O.J. Graphene based electrochemical immunosensor for the ultra-sensitive label free detection of Alzheimer's beta amyloid peptides Aβ (1-42). *Nanoscale Adv.* **2021**, *3*, 2295–2304. [CrossRef]
71. Li, Y.; Wang, Y.; Liu, X.; Feng, R.; Zhang, N.; Fan, D.; Ding, C.; Zhao, H.; Du, Y.; Wei, Q.; et al. Bifunctional pd-decorated polysulfide nanoparticle of Co_9S_8 supported on graphene oxide: A new and efficient label-free immunosensor for amyloid β-protein detection. *Sens. Actuators B Chem.* **2020**, *304*, 127413. [CrossRef]
72. Devi, R.; Gogoi, S.; Dutta, H.S.; Bordoloi, M.; Sanghi, S.K.; Khan, R. Au/$NiFe_2O_4$ nanoparticle-decorated graphene oxide nanosheets for electrochemical immunosensing of amyloid beta peptide. *Nanoscale Adv.* **2020**, *2*, 239–248. [CrossRef] [PubMed]
73. Zhang, Y.; Figueroa-Miranda, G.; Zafiu, C.; Willbold, D.; Offenhäusser, A.; Mayer, D. Amperometric Aptasensor for Amyloid-β Oligomer Detection by Optimized Stem-Loop Structures with an Adjustable Detection Range. *ACS Sens.* **2019**, *4*, 3042–3050. [CrossRef] [PubMed]
74. Kashyap, B.; Kumar, R. A novel multi-set differential pulse voltammetry technique for improving precision in electrochemical sensing. *Biosens. Bioelectron.* **2022**, *216*, 114628. [CrossRef]
75. Terbouche, A.; Lameche, S.; Ait-Ramdane-Terbouche, C.; Guerniche, D.; Lerari, D.; Bachari, K.; Hauchard, D. A new electrochemical sensor based on carbon paste electrode/Ru(III) complex for determination of nitrite: Electrochemical impedance and cyclic voltammetry measurements. *Measurement* **2016**, *92*, 524–533. [CrossRef]
76. Palsaniya, S.; Jat, B.L.; Mukherji, S. Amperometry Sensor for Real Time Detection of Hydrogen Peroxide Adulteration in food samples. *Electrochim. Acta* **2023**, *462*, 142724. [CrossRef]
77. Trevizan, H.F.; Olean-Oliveira, A.; Cardoso, C.X.; Teixeira, M.F.S. Development of a molecularly imprinted polymer for uric acid sensing based on a conductive azopolymer: Unusual approaches using electrochemical impedance/capacitance spectroscopy without a soluble redox probe. *Sens. Actuators B Chem.* **2021**, *343*, 130141. [CrossRef]
78. Zouaoui, F.; Bourouina-Bacha, S.; Bourouina, M.; Abroa-Nemeir, I.; Ben Halima, H.; Gallardo-Gonzalez, J.; El Alami El Hassani, N.; Alcacer, A.; Bausells, J.; Jaffrezic-Renault, N.; et al. Electrochemical impedance spectroscopy determination of glyphosate using a molecularly imprinted chitosan. *Sens. Actuators B Chem.* **2020**, *309*, 127753. [CrossRef]
79. Xu, J.; Zhao, C.; Chau, Y.; Lee, Y.-K. The synergy of chemical immobilization and electrical orientation of T4 bacteriophage on a micro electrochemical sensor for low-level viable bacteria detection via Differential Pulse Voltammetry. *Biosens. Bioelectron.* **2020**, *151*, 111914. [CrossRef]
80. Pizarro, J.; Segura, R.; Tapia, D.; Navarro, F.; Fuenzalida, F.; Jesús Aguirre, M. Inexpensive and green electrochemical sensor for the determination of Cd(II) and Pb(II) by square wave anodic stripping voltammetry in bivalve mollusks. *Food Chem.* **2020**, *321*, 126682. [CrossRef]
81. Abeykoon, S.W.; White, R.J. Continuous Square Wave Voltammetry for High Information Content Interrogation of Conformation Switching Sensors. *ACS Meas. Sci. Au* **2023**, *3*, 1–9. [CrossRef]
82. Xia, N.; Wang, X.; Zhou, B.; Wu, Y.; Mao, W.; Liu, L. Electrochemical Detection of Amyloid-β Oligomers Based on the Signal Amplification of a Network of Silver Nanoparticles. *ACS Appl. Mater. Interfaces* **2016**, *8*, 19303–19311. [CrossRef]
83. Singh, A.; Khatun, S.; Nath Gupta, A. Simultaneous Detection of Tyrosine and Structure-Specific Intrinsic Fluorescence in the Fibrillation of Alzheimer's Associated Peptides. *ChemPhysChem* **2020**, *21*, 2585–2598. [CrossRef] [PubMed]
84. Suprun, E.V.; Khmeleva, S.A.; Radko, S.P.; Kozin, S.A.; Archakov, A.I.; Shumyantseva, V.V. Direct electrochemical oxidation of amyloid-β peptides via tyrosine, histidine, and methionine residues. *Electrochem. Commun.* **2016**, *65*, 53–56. [CrossRef]
85. Dai, Y.; Molazemhosseini, A.; Liu, C.C. In Vitro Quantified Determination of β-Amyloid 42 Peptides, a Biomarker of Neuro-Degenerative Disorders, in PBS and Human Serum Using a Simple, Cost-Effective Thin Gold Film Biosensor. *Biosensors* **2017**, *7*, 29. [CrossRef]
86. Ding, M.; Shu, Q.; Zhang, N.; Yan, C.; Niu, H.; Li, X.; Guan, P.; Hu, X. Electrochemical Immunosensor for the Sensitive Detection of Alzheimer's Biomarker Amyloid-β (1-42) Using the Heme-amyloid-β (1-42) Complex as the Signal Source. *Electroanalysis* **2022**, *34*, 263–274. [CrossRef]
87. Li, W.; Chen, S.; Yang, Y.; Song, Y.; Ma, C.; Qiao, X.; Hong, C. Ultrasensitive electrochemical immunosensor based on the signal amplification strategy of the competitive reaction of Zn^{2+} and ATP ions to construct a "signal on" mode GOx-HRP enzyme cascade reaction. *Microchim. Acta* **2021**, *188*, 61. [CrossRef] [PubMed]
88. Wei, J.; Ge, K.; Gong, Y.; Li, L.; Tang, Q.; Liao, X.; Zhang, G.; Gao, F. DNAzyme-driven bipedal DNA walker for label-free and signal-on electrochemical detection of amyloid-β oligomer. *Int. J. Biol. Macromol.* **2023**, *228*, 234–241. [CrossRef]

89. Liao, X.; Ge, K.; Cai, Z.; Qiu, S.; Wu, S.; Li, Q.; Liu, Z.; Gao, F.; Tang, Q. Hybridization chain reaction triggered poly adenine to absorb silver nanoparticles for label-free electrochemical detection of Alzheimer's disease biomarkers amyloid β-peptide oligomers. *Anal. Chim. Acta* **2022**, *1192*, 339391. [CrossRef]
90. Garcia-Leis, A.; Sanchez-Cortes, S. Label-Free Detection and Self-Aggregation of Amyloid β-Peptides Based on Plasmonic Effects Induced by Ag Nanoparticles: Implications in Alzheimer's Disease Diagnosis. *ACS Appl. Nano Mater.* **2021**, *4*, 3565–3575. [CrossRef]
91. Le, P.G.; Kim, M.I. Research Progress and Prospects of Nanozyme-Based Glucose Biofuel Cells. *Nanomaterials* **2021**, *11*, 2116. [CrossRef] [PubMed]
92. Le, P.G.; Wu, Q.; Kong, D.Y.; Ge, J.; Il Kim, M. Tailoring Nanostructured Supports to Achieve High Performance in Enzymatic Biofuel Cells. *ACS Appl. Energy Mater.* **2022**, *5*, 13113–13127. [CrossRef]
93. Ali, A.; Zhao, J.; Khan, M.S.; Wang, H.; Ren, X.; Hu, L.; Manzoor, R.; Wu, D.; Wei, Q. Electrochemiluminescence detection for β-amyloid1-42 oligomers using silver nanoparticle decorated CuS@CoS_2 double shelled nanoboxes as dual-quencher. *Sens. Actuators B Chem.* **2021**, *329*, 129155. [CrossRef]
94. Ji, H.; Kang, X.; Yang, X.; Chen, H.; Zhu, l.; Mao, T.; He, Y.; Liu, J.; Wang, Q.; Zhou, X.; et al. Functionalized graphene-based electrochemical array sensors for the identification of distinct conformational states of Amyloid Beta in Alzheimer's disease. *Biosens. Bioelectron.* **2023**, *222*, 114927. [CrossRef] [PubMed]
95. Zhao, C.; Wang, A.; Tang, X.; Qin, J. Electrochemical sensitive detection of amyloid-β oligomer harnessing cellular prion protein on AuNPs embedded poly (pyrrole-3-carboxylic acid) matrix. *Mater. Today Adv.* **2022**, *14*, 100250. [CrossRef]
96. Yeung, S.Y.; Mucha, A.; Deshmukh, R.; Boutrus, M.; Arnebrant, T.; Sellergren, B. Reversible Self-Assembled Monolayers (rSAMs): Adaptable Surfaces for Enhanced Multivalent Interactions and Ultrasensitive Virus Detection. *ACS Cent. Sci.* **2017**, *3*, 1198–1207. [CrossRef]
97. Kumakli, H.; Hoque, A.; White, R.J. Observing Real-Time Formation of Self-Assembled Monolayers on Polycrystalline Gold Surfaces with Scanning Electrochemical Cell Microscopy. *Langmuir* **2022**, *38*, 9148–9156. [CrossRef] [PubMed]
98. Poirier, G.E.; Pylant, E.D. The Self-Assembly Mechanism of Alkanethiols on Au(111). *Science* **1996**, *272*, 1145–1148. [CrossRef]
99. Fenter, P.; Eisenberger, P.; Li, J.; Camillone, N., III; Bernasek, S.; Scoles, G.; Ramanarayanan, T.A.; Liang, K.S. Structure of octadecyl thiol self-assembled on the silver(111) surface: An incommensurate monolayer. *Langmuir* **1991**, *7*, 2013–2016. [CrossRef]
100. Soreta, T.R.; Strutwolf, J.; O'Sullivan, C.K. Electrochemically Deposited Palladium as a Substrate for Self-Assembled Monolayers. *Langmuir* **2007**, *23*, 10823–10830. [CrossRef]
101. Sosna, M.; Ferapontova, E.E. Electron Transfer in Binary Hemin-Modified Alkanethiol Self-Assembled Monolayers on Gold: Hemin's Lateral and Interfacial Interactions. *Langmuir* **2022**, *38*, 11180–11190. [CrossRef]
102. Poon, V.K.M.; Burd, A. In vitro cytotoxity of silver: Implication for clinical wound care. *Burns* **2004**, *30*, 140–147. [CrossRef] [PubMed]
103. Dowling, D.P.; Donnelly, K.; McConnell, M.L.; Eloy, R.; Arnaud, M.N. Deposition of anti-bacterial silver coatings on polymeric substrates. *Thin Solid Films* **2001**, *398–399*, 602–606. [CrossRef]
104. Li, N.; Huang, X.; Shao, H. Exploring the pH Sensitivity of Ion-Pair Interactions on a Self-Assembled Monolayer by Scanning Electrochemical Microscopy. *Langmuir* **2023**, *39*, 6529–6538. [CrossRef]
105. Ulman, A. Formation and Structure of Self-Assembled Monolayers. *Chem. Rev.* **1996**, *96*, 1533–1554. [CrossRef] [PubMed]
106. Gnauck, M.; Jaehne, E.; Blaettler, T.; Tosatti, S.; Textor, M.; Adler, H.-J.P. Carboxy-Terminated Oligo(ethylene glycol)−Alkane Phosphate: Synthesis and Self-Assembly on Titanium Oxide Surfaces. *Langmuir* **2007**, *23*, 377–381. [CrossRef] [PubMed]
107. Allara, D.L.; Nuzzo, R.G. Spontaneously organized molecular assemblies. 1. Formation, dynamics, and physical properties of n-alkanoic acids adsorbed from solution on an oxidized aluminum surface. *Langmuir* **1985**, *1*, 45–52. [CrossRef]